ARTICLE

https://doi.org/10.1590/2317-4889202120200135

BJGEO Brazilian Journal of Geology

Carbonate storm deposits and C, O isotopes of the Lagoa do Jacaré Formation (Ediacaran) in the Paraopeba area, Bambuí Group, Brazil

Marcio Vinicius Santana Dantas[1,2*], Alexandre Uhlein[1], Gabriel Jubé Uhlein[1], Alex Rodrigues de Freitas[1], Thaís Keuffer Mendonça[1], José Arthur Oliveira Santos[2], Samuel Amaral Moura Silva[1]

Abstract

A section investigated in the region of Paraopeba, Minas Gerais, provided detailed sedimentologic, stratigraphic and chemostratigraphic data from the Ediacaran Lagoa do Jacaré Formation, Bambuí Group, Southeast Brazil. This information allowed interpretation of tempestite facies in transgressive-regressive cycles, reinforcing the previously proposed storm-influenced sedimentation model and clarifying how it is associated with unusually high C-isotope values related to the Middle Bambuí Excursion (MIBE). Facies analysis of nine lithofacies identified at the GMD quarry based on field and petrographic descriptions showed distal tempestite facies grading upwards to a shallower, oncoidal/ooidal carbonate marine environment, then to basinal shales. The entire succession comprises a low-order transgressive hemicycle, recording the transition from a storm-influenced carbonate ramp to a siliciclastic-dominated platform. Chemostratigraphic data yielded high $\delta^{13}C$ values ranging between +11.11‰ and +13.94‰. Our data contribute to the revision of the previously proposed interpretation and as well as to the understanding of paleoenvironmental conditions and C isotope signatures across the MIBE, near the Ediacaran-Cambrian boundary in the Bambuí Basin.

KEYWORDS: Bambuí Group; Lagoa do Jacaré Formation; stratigraphy; chemostratigraphy; ediacaran.

INTRODUCTION

The Bambuí Group is one of the most researched Neoproterozoic basins worldwide, representing the main cover of the São Francisco craton in central Brazil. Important studies have been conducted in the last few years, mainly due to its highly positive C excursion, previously described as MIBE (Middle Bambuí positive Excursion) by Uhlein *et al.* (2019), which can reach $\delta^{13}C$ values as high as +15‰ (Martins and Lemos 2007, Santana 2011, Reis 2013, Paula-Santos *et al.* 2015, Hippert *et al.* 2019, Cui *et al.* 2020, Caetano-Filho *et al.* 2021). More and more studies are being performed on the cause behind these high values and it is currently hypothesized that a local carbon cycle anomaly triggered by methane emissions to the atmosphere oversees such $\delta^{13}C$ positive anomaly (Cui *et al.* 2020, Caetano-Filho *et al.* 2021). Therefore, it is a primary necessity to properly characterize the stratigraphic patterns and depositional settings generated in this epicontinental basin with such a unique biochemical condition. However, there is a historical lack of detailed sedimentological and stratigraphic investigations on the other units, mainly the Lagoa do Jacaré Formation.

The Bambuí Group is also an important succession since its geological record contributes to the understanding of the Neoproterozoic glaciation events (Snowball Earth of Hoffman *et al.* 1998), the fragmentation of Rodinia and amalgamation of Gondwana supercontinents (Condie 2016), as well as the evolution of Ediacaran marine environments (Johnston *et al.* 2012, Li *et al.* 2016). Many authors have been worked with C, O, Sr and S isotopes and lithochemical data for years, providing insights on the evolution of this neoproterozoic succession (Alvarenga *et al.* 2007, Babinski *et al.* 2007, Sial *et al.* 2009, Caxito *et al.* 2012, Vieira *et al.* 2015, Kuchenbecker *et al.* 2016, Sial *et al.* 2016, Paula-Santos *et al.* 2017, Uhlein *et al.* 2019 among others), especially aimed in the cap carbonate succession of the Sete Lagoas Formation.

In this way, we present detailed sedimentological and stratigraphic data that serve as a basis for carbon and oxygen isotope discussion of an outcrop in the region of Paraopeba, central Minas Gerais, Brazil (Fig. 1). Carbonate lithofacies are also present and discussed along with field, well log, and isotope data, contributing to the understanding of the processes involved in the deposition of the Lagoa do Jacaré carbonates

[1]Programa de Pós-Graduação em Geologia, Instituto de Geociências, Centro de Pesquisas Professor Manoel Teixeira da Costa, Universidade Federal de Minas Gerais – Belo Horizonte (MG), Brazil. E-mails: márcio_ufs08@hotmail.com, auhlein@gmail.com, guhlein@gmail.com, lecaorf@gmail.com, thaiskmendoca@gmail.com, amaralms.samuel@gmail.com

[2]PROGEOLOGIA Laboratory, Núcleo de Competência em Petróleo e Gás de Sergipe, Universidade Federal de Sergipe – São Cristóvão (SE), Brazil. E-mail: arthur.geol@hotmail.com

*Corresponding author.

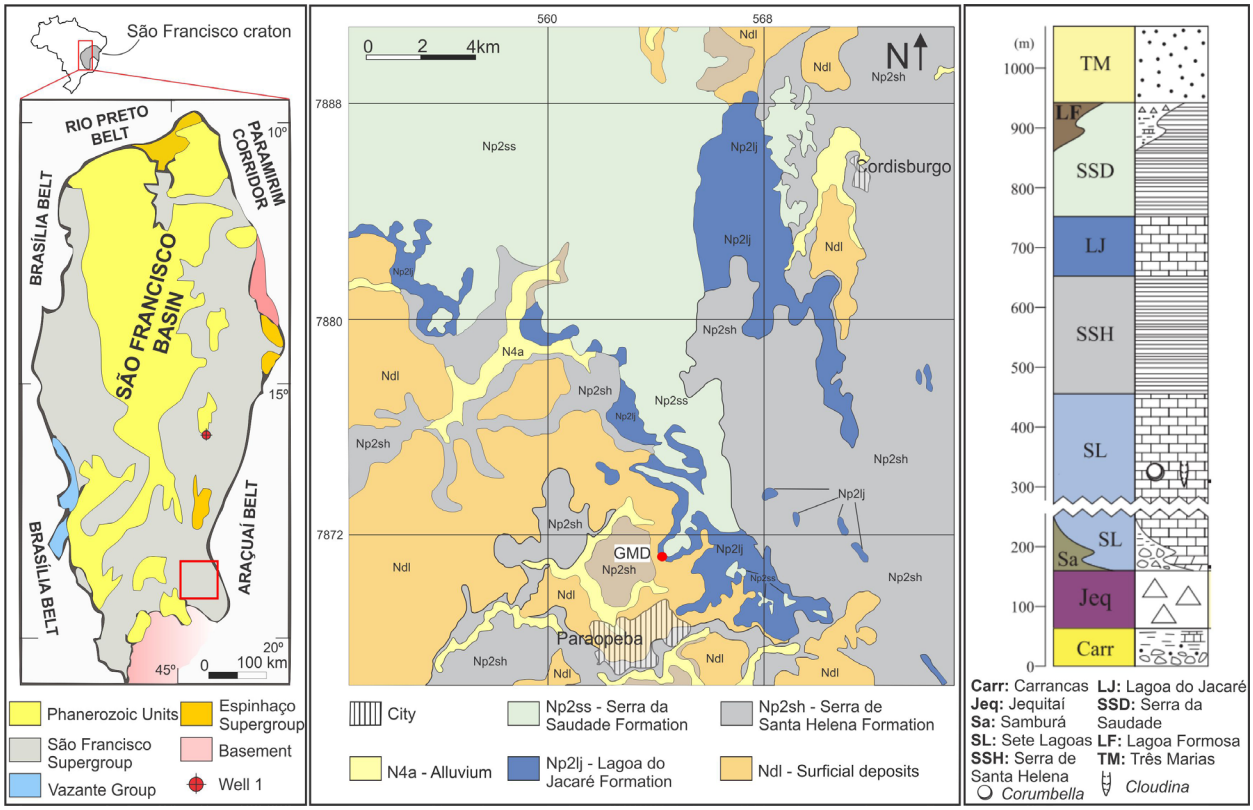

Figure 1. Geological map of the studied area and general stratigraphic column of the Bambuí Group. Based on the Sete Lagoas geological map by Tuller (2010) and Alkmim and Martins-Neto (2001). Stratigraphic chart from Uhlein et al. (2017).

as well as proposing new interpretations to what is currently considered.

Geological settings of the São Francisco Basin and Bambuí Group

The Bambuí Group corresponds to the post-glacial sequence of the São Francisco Supergroup (Megasequence by Martins and Lemos 2007). It is limited by two orogens or fold-thrust belts: the Brasília Belt to the west and the Araçuaí Belt to the east (Dardenne 2000, Zalán and Romeiro-Silva 2007, Reis and Alkmim 2015). The Bambuí Group comprises carbonate rocks intercalated with shales and sandstones deposited in a foreland type basin (Dardenne 2000, Martins-Neto *et al.* 2001, Coelho *et al.* 2008). Its role as a foreland basin during the rising of the Brasília Belt (650-600 Ma) during the Brasiliano orogenic event (Castro and Dardenne 2000, Dardenne 2000, Martins-Neto *et al.* 2001, Rodrigues 2008, Pimentel *et al.* 2011, Reis *et al.* 2017, Uhlein *et al.* 2017) is still discussed, even though recent geochronological data claims much younger ages (Warren *et al.* 2014, Paula-Santos *et al.* 2015, Moreira *et al.* 2020). Alkmim and Martins-Neto (2001) divided the Bambuí Basin in three sectors or structural domains: western, where the rocks yield to the influence of the Brasília Belt tectonics and present folds and thrusts; eastern domain, with folds and thrusts influenced by the Araçuaí Belt; and central domain, where the layers are mainly undeformed.

The Bambuí Group represents an Ediacaran-Cambrian succession deposited in marine environments at the base, grading upward to a fluvial-deltaic-marine environment at the top (Martins and Lemos 2007, Zalán and Romeiro-Silva 2007, Alvarenga *et al.* 2012, Paula-Santos *et al.* 2015, Uhlein *et al.* 2019, Moreira *et al.* 2020). It represents a mixed carbonate-siliciclastic sedimentation deposited by clear transgressive (shales) and regressive (carbonate rocks) cycles (Dardenne 1978, Martins and Lemos 2007, Alkmim and Martins-Neto 2012). Its lithostratigraphy is divided in six formations according to Dardenne (1978, 2000): Jequitaí Formation, mainly formed by diamictites, rare sandstones and rhythmites; Sete Lagoas Formation, composed of a succession of dolomites and carbonates; Serra de Santa Helena Formation, presenting shales and siltstones with carbonate lenses; Lagoa do Jacaré Formation, alternating dark carbonates (sometimes ooidal) with siltstones and marls; Serra da Saudade Formation, composed of shales, sandstones and green claystones; Três Marias Formation, presenting arkosic sandstones and siltstones. Regionally, from the central basin areas to the eastern sector, the Lagoa do Jacaré Formation outcrops as sparse occurrences (Fig. 1). According to Dardenne (1978), it is composed of ooidal and pisoidal carbonate lenses, fetid when broken apart, usually presenting storm-influenced sedimentary structures, intercalated with marl, sandstone and siltstones. Microbialites also occur (Fragoso *et al.* 2011, Uhlein *et al.* 2019) in sparse outcrops. The main depositional environment of the Lagoa do Jacaré Formation is interpreted as shallow marine, influenced by tidal waves (fair and storm weather) and currents (Martins and Lemos 2007, Reis and Suss 2016, Uhlein *et al.* 2019). More recently, Freitas *et al.* (2021) has detailed the lithofacies and depositional model of the Lagoa do Jacaré Fm. in an outcrop located at the central part of the basin.

Several attempts to define its stratigraphic framework were made since Dardenne (1978). Using seismic and well logs, Martins and Lemos (2007) defined four 3rd-order depositional sequences separated by unconformities marked by faciological discontinuities and strong isotopic breaks that comprise the São Francisco Megasequence, described as following: Glacial marine (sequence 1- Jequitaí Formation); progradational distal steepened carbonate ramp (sequence 2- Sete Lagoas Fm.); carbonate-siliciclastic homoclinal ramp (sequence 3- Serra de Santa Helena Fm., Lagoa do Jacaré Fm.); and mainly siliciclastic shallow marine progradational platform (sequence 4- Serra da Saudade Fm. and Três Marias Fm.). More recently, Reis *et al.* (2013) and Uhlein *et al.* (2017) presented 2nd-order stratigraphic cycles for the Bambuí Group sedimentary succession using different methods. The former recognized four 2nd-order shallowing upward sequences, while the latter recognized five 2nd-order transgressive-regressive sequences.

Concerning isotope geochemistry, since the mid 2000's, many isotopic data had been gathered in different parts of the basin, as mentioned above, in order to correlate its deposition with the Marinoan or Sturtian glaciations (Babinski *et al.* 2007), in addition to the better understanding of its evolution during the boundary between Neoproterozoic and Cambrian (Santos *et al.* 2004, Alvarenga *et al.* 2012). Currently, it is well known that the cap carbonate from the base of the group starts with negative values of $\delta^{13}C$ (Caxito *et al.* 2012, Paula-Santos *et al.* 2015) in the order of -4,5‰, grading upward to extremely positive values at the top of Sete Lagoas Formation (+8‰, +10‰) and in the Lagoa do Jacaré Formation (+14‰, +15‰) (Iyer *et al.* 1995, Santos *et al.* 2000, Uhlein *et al.* 2017). The causes for this isotopic behavior are under investigation but may correspond to a regional rather than global carbon cycle anomaly (Uhlein *et al.* 2019, Cui *et al.* 2020, Caetano-Filho *et al.* 2021).

Attempts of dating the Bambuí Group started back in the 1980's using different methods (Cloud and Dardenne 1973, Cordani *et al.* 1978, Parenti-Couto *et al.* 1981). In the last 20 years, much of the discussion spun around the question of whether the Bambuí Group was the aftermath of the early Cryogenian (Sturtian) or late Cryogenian (Marinoan) glaciations (e.g., Alvarenga *et al.* 2007, Caxito *et al.* 2012) More recently, geochronological and paleontological studies concerning the depositional age of the Bambuí suggest a depositional age spanning through the Ediacaran and Cambrian periods (Warren *et al.* 2014, Paula-Santos *et al.* 2015, Uhlein *et al.* 2017, 2019, Moreira *et al.* 2020).

METHODS

Fieldwork campaigns were carried in a disabled quarry (named GMD; location 564131/ 7871233 UTM 23K) in the vicinities of Paraopeba, central Minas Gerais (Fig. 1). We described a 125 m-thick vertical composite section at the location using standard field methodology description and yielding detailed sedimentological and stratigraphic data (Figs. 2 and 3). Twenty-nine (29) samples were collected in order to perform C and O isotopic analysis. We also made 23 thin sections of the main intervals. The lithofacies were described according to the Dunham (1962) and Embry and Klovan (1971) classifications and the results are in accordance with Freitas *et al.* (2021). Sequence stratigraphy was described following concepts defined by Embry and Johannessen (1993) and Zecchin and Catuneanu (2017). We interpreted two GPR profiles collected with a 160 MHz frequency antenna using the Mala Ground Explorer. They were set perpendicular and longitudinal to the outcrop in order to identify the different geometries of the layers. Data processing using the ReflexW software comprised time-zero adjustment, background removal, band-pass frequency filters and gain equalization.

Isotopes analyses were performed at NEG-LABISE in the Universidade Federal de Pernambuco, according to the following method: 20 mg of powdered sampled was used for the extraction of CO_2 gas. The powder reacted with the orthophosphoric acid (H_3PO_4) at 25°C to release CO_2. The gas was then analyzed in a Thermofinnigan Delta V Advantage mass spectrometer and the results were expressed in δ per mil (‰), normalized to the VPDB (Vienna Pee Dee Belemnite) e V-SMOW standards for $\delta^{13}C$ and $\delta^{18}O$ respectively, with precision higher than $\pm$ 0,1‰.

RESULTS

Facies and stratigraphy

The composite vertical profile is composed of two vertical profiles (Figs. 2 and 3): one in detail for better understanding of the facies occurrence inside the quarry (GMD quarry, 26 m thick) and another (125 m thick) in the vicinities that encompass the former, therefore presenting a thicker interval of the Lagoa do Jacaré Formation. In general, the GMD quarry is mainly composed of carbonate breccias intercalated with finer facies such as grainstone, wackestone, mudstone, and siltstone (Fig. 4). The breccias generally present a lenticular geometry and erosive base and are composed of intraclasts of mudstone with diverse shapes and sizes, oriented or chaotically distributed (Fig. 4B). The bed thickness ranges laterally from 5 to 20 cm, showing grading bedding, tabular cross-stratification and massive structures. Grey to dark grey, fine- to coarse-grained grainstone beds (up to 20 cm-thick) are recurrent facies that present hummocky cross-stratification (HCS) (Fig. 4F), planar and trough cross-lamination, planar cross-stratification and wave ripples, likely deposited by oscillatory, unidirectional and combined flows (Fig. 4D). Some grainstones may present few mudstone intraclasts. Sparse dark grey massive siltstone with parallel lamination and wackestone with syneresis cracks (Fig. 4C) occur between grainstones and breccias. Toward the top and completing the composite section, there is an increase in pisolitic-oncoidal rudstone (Figs. 4A and 4E), fine sandstone and mudrock beds. A detailed description of the lithofacies and their sedimentary structures can be found in Table 1 and illustrated in Figure 4.

GPR profile interpretations have provided results on the depositional geometry of lithofacies (Fig. 5), an important

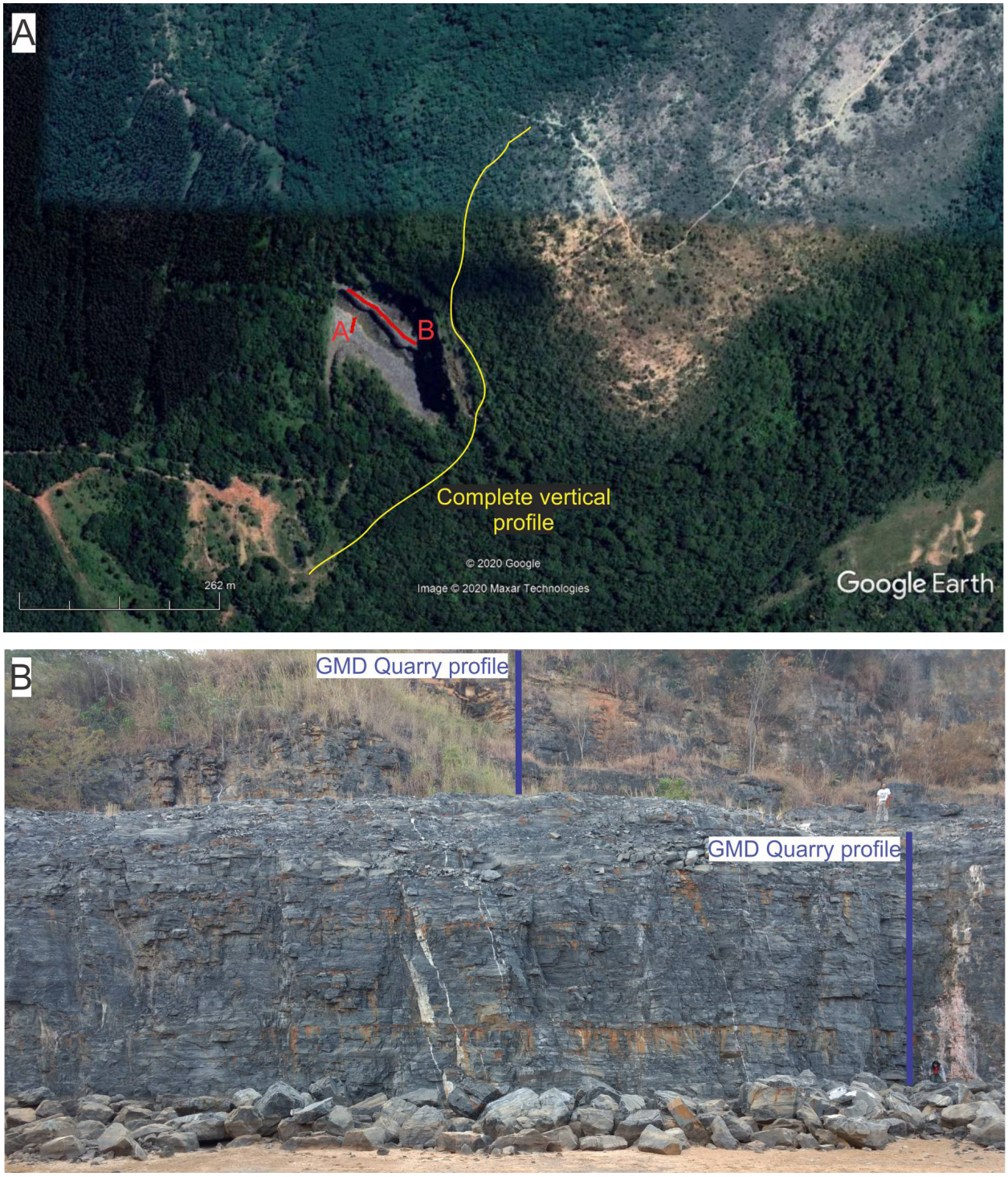

Figure 2. The GMD quarry: (A) Google Earth image presenting the location of the GPR profiles in red and the trail of the surrounding profile in yellow; (B) location of the detailed vertical lithological profile inside the quarry (blue lines).

aspect to unveil depositional systems. A diagnostic geometry identified is the progradational pattern of the radarfacies, as the hummocky and sigmoidal types seen in profile B in NW-SE direction (see location of the profiles in Fig. 2). They represent the migration of large wave ripples in the offshore/shoreface transitional environment during storm events. From the direction of the GPR profile B, cross-stratification structures migrate to SE. In the N-S direction, the main radarfacies is the parallel stratification, as seen in profile A, with the beds showing great lateral continuity, and in accordance with field observations. Those radarfacies are related to low energy events, such as deposition by suspension in the mid and outer ramp after storm events.

Petrographic analysis has provided detailed descriptions of the carbonate lithofacies and consequently the differentiation of the main components and identification of major diagenetic features (Fig. 6). We agree with the lithofacies proposed by Freitas *et al.* (2021) at the first part of the GMD outcrop and extend it to the entire section, coupled with new ones. We briefly present their characteristics as follow: main allochemical components are micro-oncoids (Fig. 6C), oncoids and ooids, present in oncoidal-ooidal intraclastic grainstone (oiG).

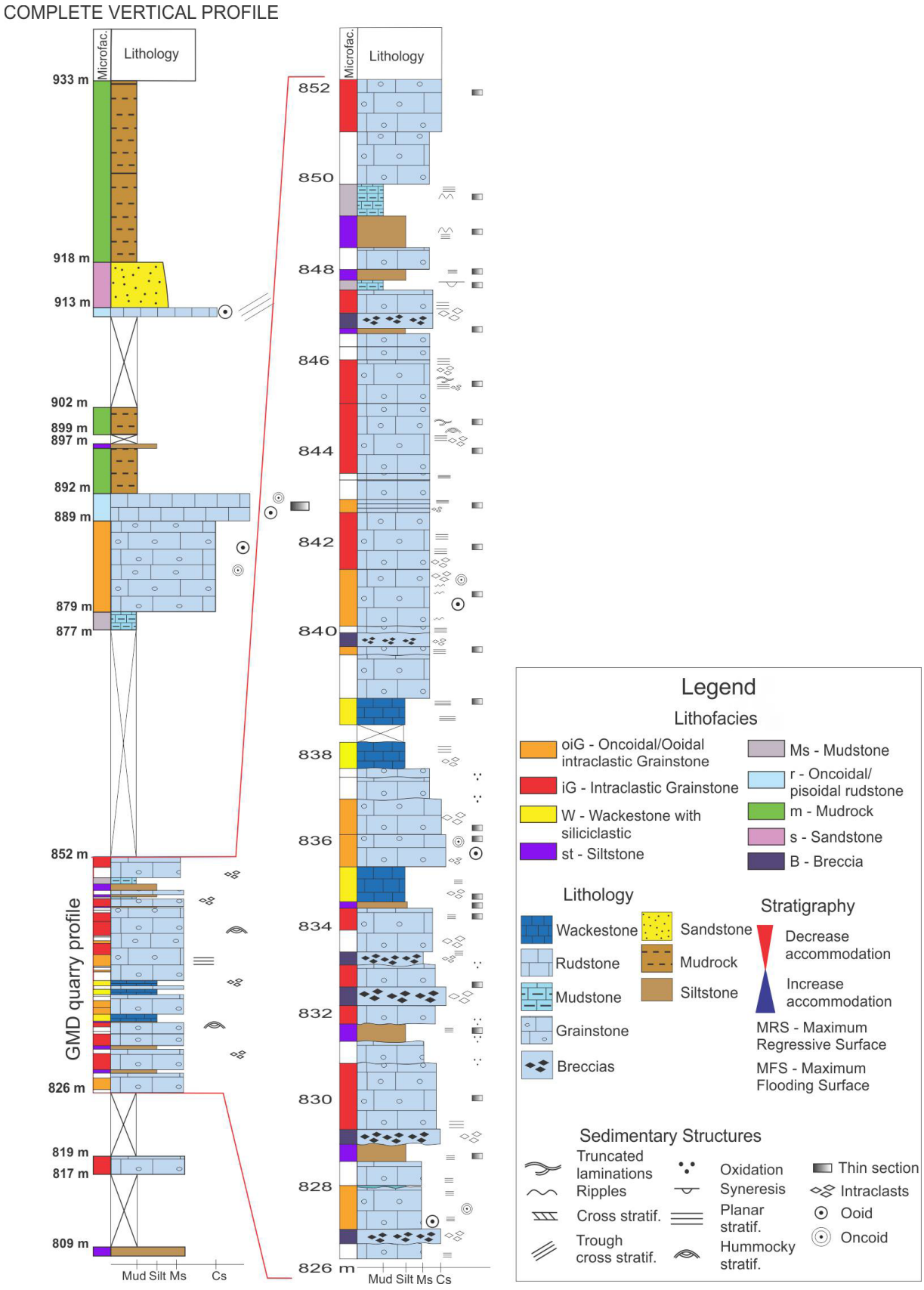

Figure 3. Vertical profiles of the GMD quarry and its surroundings (125 m-thick) presenting the main sedimentary structures, lithologies and lithofacies interpreted. Symbol description can be found in Fig. 10.

The intraclastic grainstone (iG) has similar textural aspects to oiG without significant coated grains. Instead, intraclasts are up to 2 mm, making up to 50% of the allochemical components and are often micritized. Oncoidal-pisoidal rudstone (r) has pisoids and oncoids as main components, with predominantly equant calcite cement in a loose packing. Wackestone with siliciclastic extraclasts (W) (Fig. 6D) and mudstones (Fig. 6E) (Ms) are the finest grained lithofacies. A distinct characteristic of the GMD quarry is the presence of siliciclastic content in all lithofacies, even in the carbonate facies. Siltstone (st)

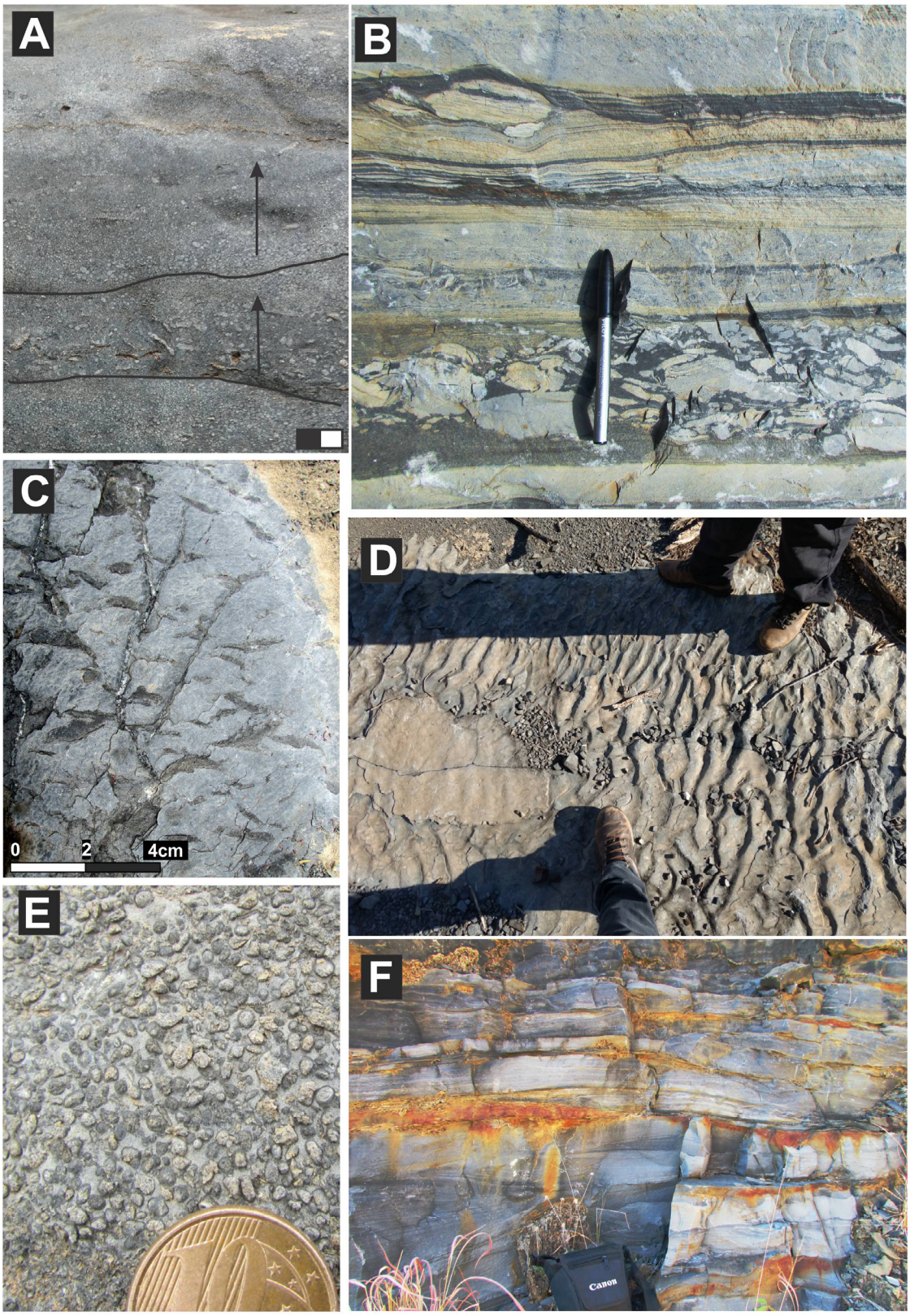

Figure 4. Main lithofacies and their sedimentary structures in the GMD quarry. (A) Detail of oncoidal/ooidal intraclastic grainstone with erosive contacts and graded beds. (B) Non-oriented, normally graded breccias grading up to fine to medium grainstones and siltstones. (C) Syneresis cracks in wackestone. (D) Current ripples in fine to medium grainstone. (E) Detail of oncoidal-pisoidal rudstone. (F) Coarse grainstone with hummocky cross-stratification.

(Fig. 6F) presents more than 50% of siliciclastic grains with some carbonate micrite (< 20%). We described only macroscopic aspects of the breccia (B), as well as the siliciclastic facies, mudrock (m) and sandstone (s) at the top of the section. Detailed lithofacies description can be seen in Table 1.

Diagenetic features were described in order to evaluate possible C and O isotopic alterations. In general terms, early diagenesis plays the most important role in the diagenetic evolution of the carbonates in the GMD quarry. Micritization of intraclasts, ooids, and oncoids is easily observed (red arrows

Table 1. Main lithofacies described in the outcrop of the GMD quarry and surroundings and their interpretation.

Lithofacies	Description	Petrographic aspects	Depositional process	Interpretation
Oncoidal-ooidal intraclastic grainstone (oiG)	Dark grey, massive, laminated, with wave ripple or HCS, laminations and cross stratifications. Lenticular or tabular geometry. Micritized micro-oncoids, oncoids and ooids are present. Cm- to m-thick.	Fine grained (0,076 to 0,32 mm), fine blocky calcite cement (20-70%), ooids/ peloids (30-65%), angular to subrounded intraclasts (< 40%), quartz (5-10%) and 1% average of opaque minerals. Some mica can be present. Peloids/ooids and micritized micro-oncoid are 0,14 to 0,35 mm and commonly subrounded to rounded, occasionally presenting "ghosts" of concentric structure. Plane parallel lamination. Micritization and pyritization processes.	Oscillatory or combined flows with high to low energy.	Storm events in mid to outer ramp.
Intraclastic grainstone (iG)	Dark grey, massive, laminated, with wave ripple or HCS, laminations and cross stratifications. Lenticular or tabular geometry. Intraclasts are the main component. Cm- to m-thick.	Commonly laminated, grain size between silt and medium sand (0,028 – 0,35 mm). In general, 40-70% blocky calcite cement content, 10-50% of mudstone intraclasts. Intraclasts are up to 2 mm, angular to subangular, sometimes with elongated shape. Micas are present (< 5%). Ooids and micro-oncoids are rare, poorly preserved.	Oscillatory or combined flows with high to low energy.	Storm events in mid to outer ramp.
Breccia (B)	Intraclasts of mudstone with diverse sizes and shapes oriented or chaotically distributed in a carbonatic matrix. Sharp contact or erosive base. Mainly lenticular geometry.	-	Erosive process. Turbulent and high energy flow.	Storm events in mid to outer ramp.
Wackestone with siliciclastic (W)	Fine, light grey, generally massive, eventually laminated. Intraclasts and siliciclastic grains may be present (< 15%).	Silt to fine grained carbonate with siliciclastic grains. Generally laminated. Carbonate matrix (50-70%), angular to subangular quartz grains (15-50%), mudstone intraclasts (< 15%), opaques (< 15%), white micas (< 5%), rarely clay minerals and feldspar.	Suspension, low energy.	Deposition by suspension and precipitation in protected area or outer ramp.
Mudstone (Ms)	Fine, massive to poorly laminated, rare siliciclastic content (< 10%). Syneresis cracks.	Carbonate rock with 5-10% of siliciclastic content (grains of quartz, mica and opaque minerals).	Suspension, low energy.	Deep marine, outer ramp.
Oncoidal-pisoidal rudstone (r)	Dark grey. Oncoids and pisoids with intraclasts. Tabular cross-stratification. Lenticular geometry.	Oncoids, pisoids, ooids, rare intraclasts, sparry calcite cement predominates.	Unidirectional tractive flow, moderate to low energy.	Sand bars in inner ramp.
Siltstone (st)	Dark grey, massive or plane parallel lamination.	Medium to coarse silt (0,034 - 0,056 mm), laminated. Composed mainly of angular to subangular quartz grain (50-85%), surrounded by carbonate cement, oriented mica, cloritized clay matrix and disperse opaque (5-10%). Few carbonate matrix (< 20%)	Low energy, suspension	Deep marine, outer ramp to basin.
Mudrock (m)	Massive, brown. Fine laminated, with tabular geometry. Cm- to mm-thick beds.	-	Suspension, low energy.	Deep marine sedimentation, outer ramp to basin.
Sandstone (s)	Fine, light brown, massive.	-	High-energy tractive flow	Shoreface to foreshore (?)

in Fig. 6C) and the texture of the grains is altered to a massive, brown colored, sometimes shapeless, different from cement and matrix (Dias-Brito 2017) (Figs. 6B and 6C). When the process is more intense, it transforms the grains into peloids. Fringes around the coated grains are observed in lithofacies oiG, iG and r (Figs. 6A and 6B). Sparry calcite, equant calcite and drusy cements are second and occasionally third phases of cementation, filling almost all the remaining porosity (Figs. 6B, 6G and 6H). The geopetal feature in Figure 6H presents examples of these cements. Pyrite precipitation is

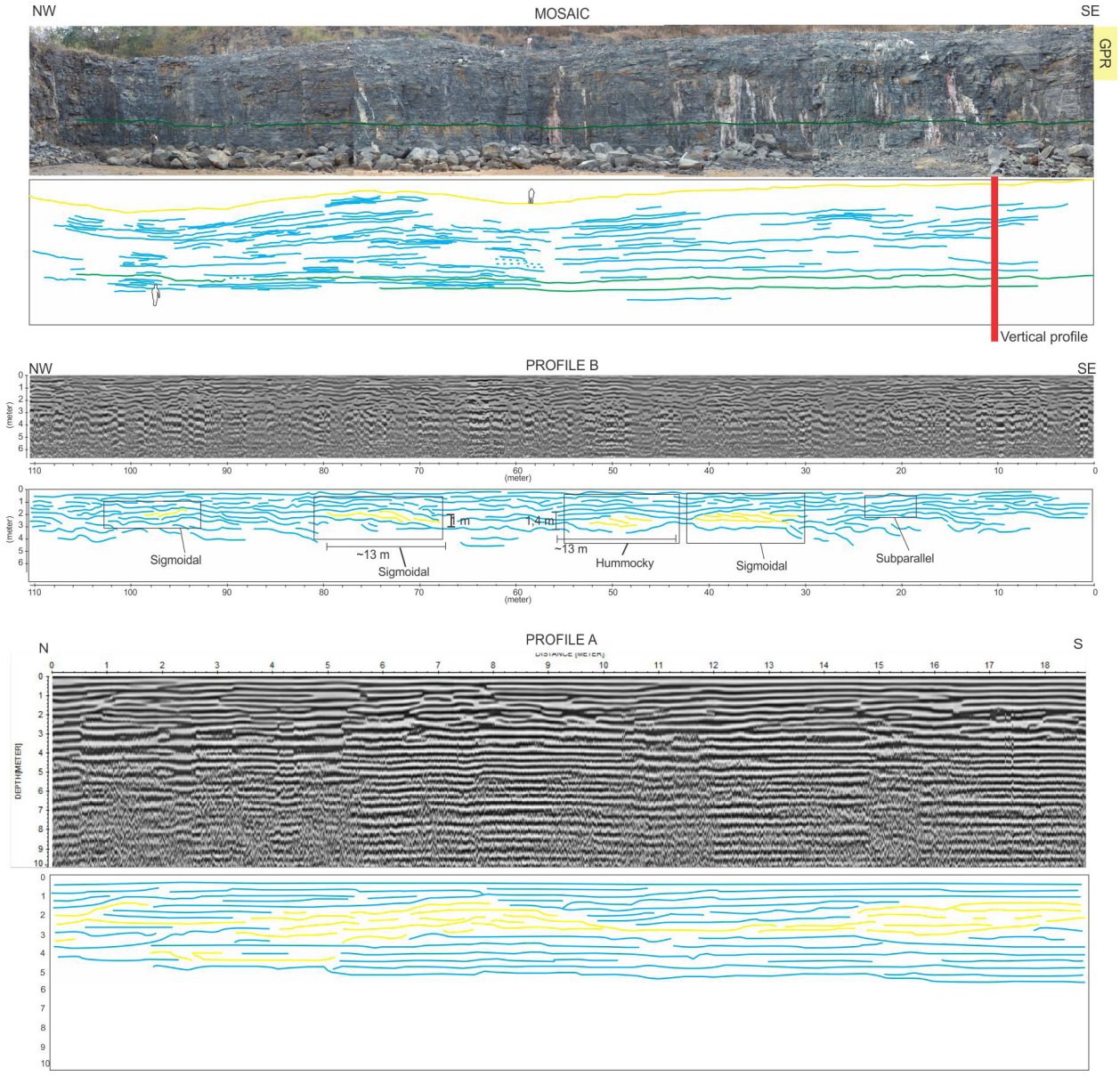

Figure 5. GPR profiles and mosaic of the outcrop and their interpretations. Beds interpreted on the mosaic. In the GPR profiles, note the progradational geometry (yellow lines) to SE in parallel to outcrop profile B and the predominant plane-parallel geometry in the transversal profile A.

also an important digenetic process, suggesting active sulfate and iron cycles in sediment pores. During early or late diagenesis (Taylor and Macquaker 2000), pyrite substitutes the organic matter present in the micro-oncoids and oncoids, as seen in Figure 6B.

Recrystallization processes occur in burial environment during mesodiagenesis. In Figure 6B we can see recrystallized crystals have been part of an oncoid and the cement at the same time. With a progressive burial, stylolites and seams are formed via chemical compaction (Fig. 6C) (Flügel 2010). At this level, it is possible to develop sutured grain contact and fracturing of the grains (Fig. 6G). Microfractures also develop during compaction on this phase (Fig. 6E) and dissolution processes are almost inexistent. Only one feature was found and its textural relationship is difficult to understand (Fig. 6I). All characteristics of lithofacies and their interpretations are summarized in Table 1, and some photomicrographs can be found in Figure 6.

DISCUSSION

Facies interpretation and sequence stratigraphy

The lithofacies described in the GMD quarry suggest deposition in a marine carbonate environment, often influenced by storm and fair-weather waves. The widespread high-frequency intercalation of grainstones with hummocky cross-stratification (HCS), truncated laminations, wave ripples and mud intraclasts suggest a mid-ramp sedimentation or lower to middle shoreface deposits (Fig. 3). These facies are recurrently positioned in a predictive arrangement and likely make up episodic storm-deposited beds, often named tempestites (Brenchley 1985, Einsele 1992, Myrow and Southard 1996, Flügel 2010, Pérez-López and Pérez-Valera 2012) (Fig. 7). They represent a class of event deposits, resulting of short-term sedimentation processes that produce characteristic sedimentary signatures (Flügel 2010). Tempestites or storm-deposited beds represent

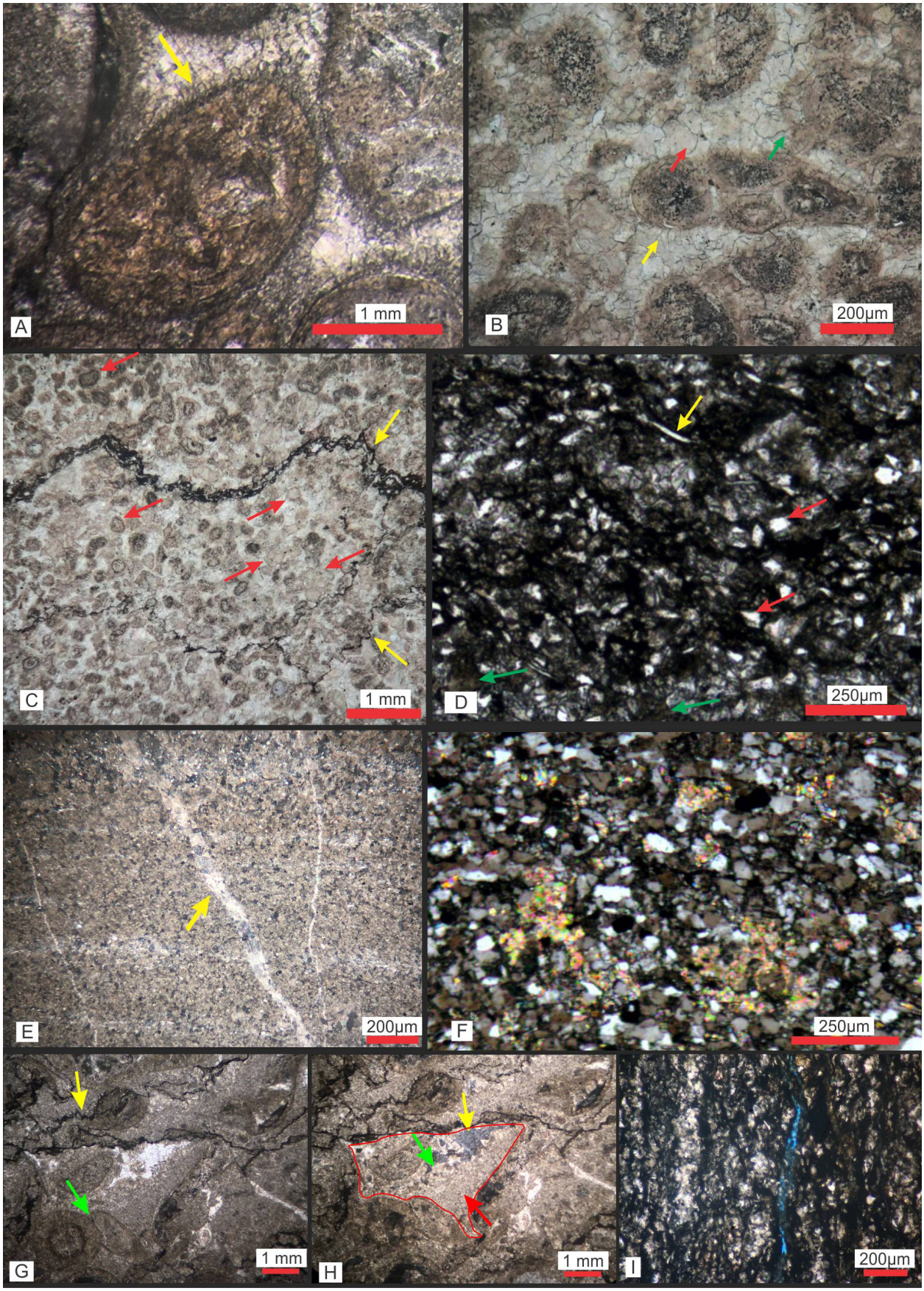

Figure 6. Lithofacies studied in the GMD quarry and main diagenetic features. (A) Detail of a fringe in an oncoidal-pisoidal rudstone. (B) Poor fringe pointed by yellow arrow, equant calcite cement pointed by the red arrow and an example of recrystallization (green arrow) in an oncoidal grainstone. Note pyrite dissemination inside oncoids. (C) Micro-stylolites (yellow arrows) and intraclasts and micritized micro-oncoids pointed by red arrows in an oncoidal/peloidal grainstone. (D) Wackestone with high siliciclastic extraclasts (quartz and mica, red and yellow arrows respectively) content, general view. Matrix pointed by the green arrow; (E) Mudstone, microfractures in detail. (F) Quartz grains in siltstone with some limestone cement (high birefrigence). (G) Sutured contacts and stylolite indicated by green and yellow arrow respectively (PPL). (H) Geopetal feature: recrystallization of matrix, equant calcite and drusy calcite indicated by red, green and yellow arrows respectively (XPL). (I) Micro dissolution feature.

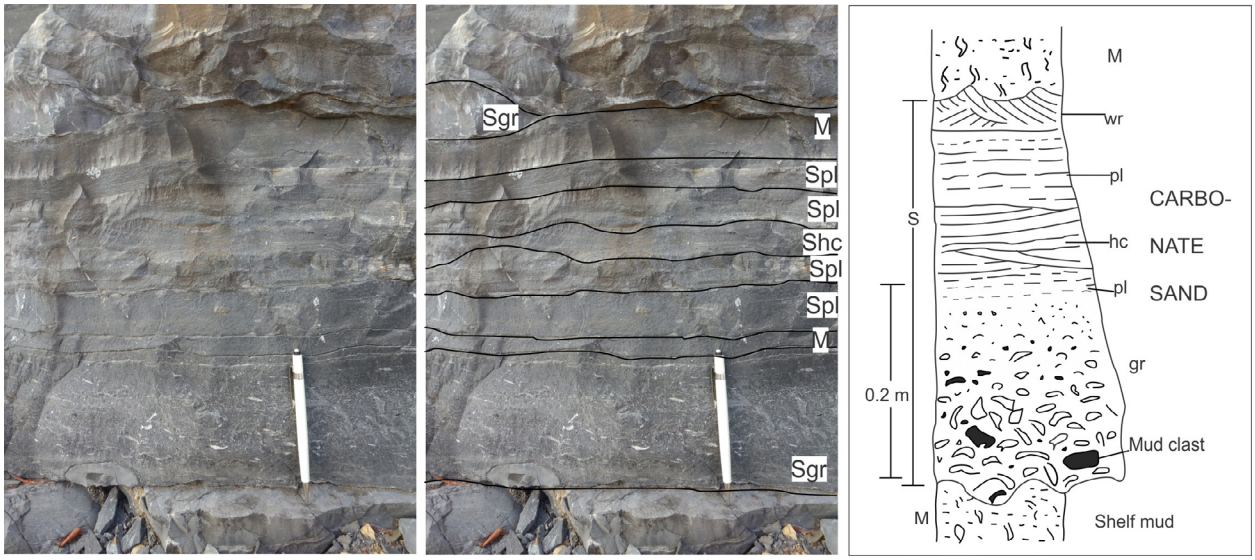

Figure 7. Interpretation of a tempestite cycles that outcrops in the GMD quarry (center image) as described by Einsele (1992) (sketch on the right) resulting of consecutive storms events throughout time. Codes used in the sketch: Wave ripples and wave ripple cross-stratification (Swr) - Low-angle hummocky cross-stratification (Shc) - Parallel lamination and current ripple cross-stratification (Spl) - Graded layer with basal lag deposit (Sgr) - Normal shelf mud, intensely bioturbated (M).

the deposition of carbonate or siliciclastic sediments reworked during successive storm events and deposited across the shelf as the storm decreases in energy. Fining-upward and varying sedimentary structures along successive beds are related to decreasing energy conditions (Aigner 1985). Storm bottom currents, which eroded carbonate sediments from shallower environments, deposited the carbonate grains, mud intraclasts and ooids in the lower to middle shoreface and likely formed a large portion of the beds of the GMD quarry. Some works have detailed the expected structures from storm-dominated sedimentation in carbonate settings (Molina *et al*. 1997, Mohseni and Al-Aasm 2004, Pérez-López and Pérez-Valera 2012). Mud intraclasts (or shells in the Phanerozoic) occur at the base of the bed and are formed during the higher energy moments of the storm; when the waves cause erosion reaching the seabed (Sgr from Einsele 1992 tempestite model showed in Fig. 7). According to Flügel (2010), some erosive structures are difficult to recognize in ancient carbonate facies due to bioturbation (not the case of Precambrian units) and diagenetic overprint. As the storm's energy decreases and the sedimentation continues, this facies grades upward to grainstones with parallel lamination, hummocky cross-stratification, and horizontal wave-ripple lamination (Spl, Shc, Swr in Fig. 7). Finer sediments, such as mudstone and wackestone, deposited by suspension during the lowest energy phases represent the upper part of the tempestite cycle (Einsele 1992, Nichols 2009, Flügel 2010). The record of significant and recurrent wave action on the sea floor and evidence of deposition by decreasing flow energy are good diagnostic markers of tempestites, although care must be taken since the facies in a tempestite bed may vary widely. When the time between storm events is long enough, hardgrounds and/or background sedimentation may occur, developing surfaces with calcite and/or ferric and ferrous iron cementation, as well as the deposition of mudstones with syneresis and siltstones (Fig. 4C). Recent weathering results in oxidation of the hardground layers containing iron minerals represent a stratigraphic-controlled feature, as seen in some parts of the outcrop (Fig. 2).

Overall, it is possible to correlate each lithofacies described in the GMD quarry to the facies predicted in tempestite intervals. Breccia (B) lithofacies are set at the base of the cycle, deposited by the higher energy conditions of the storm. This facies is related to the erosion process and to the generation and redeposition of cm-sized mudstone intraclasts that constitute the breccia beds. Lithofacies oiG and iG correspond to a waning of the storm and are deposited in the middle part of the tempestite cycle. They comprise stratified grainstones (Shc, Spl, Swr) of intermediate energy with micro intraclasts, micro oncoids and peloids that vary laterally and vertically between each other (Fig. 7). W, s and m represent the top of the tempestites and are related to the low energy (suspension) sedimentation process after the end of each storm event. All interpretations and correlations between theoretical lithofacies and lithofacies are summarized in Figure 8.

This general order of sedimentation can be altered if storm events occur repeatedly, and it is necessary to consider the lateral facies distribution in these cycles. Indeed, it is rare to identify the complete sequence of facies of one tempestite, and the oiG and iG lithofacies (or any other lithofacies) could continue to present one after the other. Pérez-López and Pérez-Valera (2012) observed this process in the Triassic carbonate tempestite where the deposits were composed of coarse-grained basal facies capped by mudstones. This phenomenon is known as cannibalism or amalgamation (Aigner 1985, Einsele 1992), and it occurs when the upper parts of pre-existing thick tempestites are reworked by storms of particularly high erosional capacity. The left image in Figure 7 shows the best tempestite cycle seen in an outcrop and its interpretation in the central image, in comparison with the ideal tempestite defined by Einsele (1992) on the right.

The predominance of each lithofacies in the geological record is a clue to the prevalence of proximal and distal depositional

Tempestite Facies (Einsele, 1992)	Lithofacies (this work)	Components	Structures/ Texture
Sgr - Graded or not graded with basal lag deposit. Erosional base with sole marks (in places bipolar or multi-directional	Breccias	cm-sized Intraclasts Carbonate cement	Massive or oriented tabular cross-stratification normal grading
Shc - Low angle hummocky cross-stratification	Oncoidal-ooidal Grainstone	micritized oncoids ooids mm-sized Intraclasts Cement	HCS - Hummocky cross-stratification
Shc - Low angle hummocky cross-stratification	Intraclastic grainstone	mm-sized Intraclasts Cement	HCS - Hummocky cross-stratification
Spl Parallel lamination and current ripple cross-stratification	Wackestone	Rare intraclast Micrite	laminated few intraclasts
Sm/M - Normal or redeposited shelf mud	Mudstone	Micrite	massive syneresis cracks
Sm - redeposited shelf silt	Siltstone	Siliciclastic silt	massive or laminated

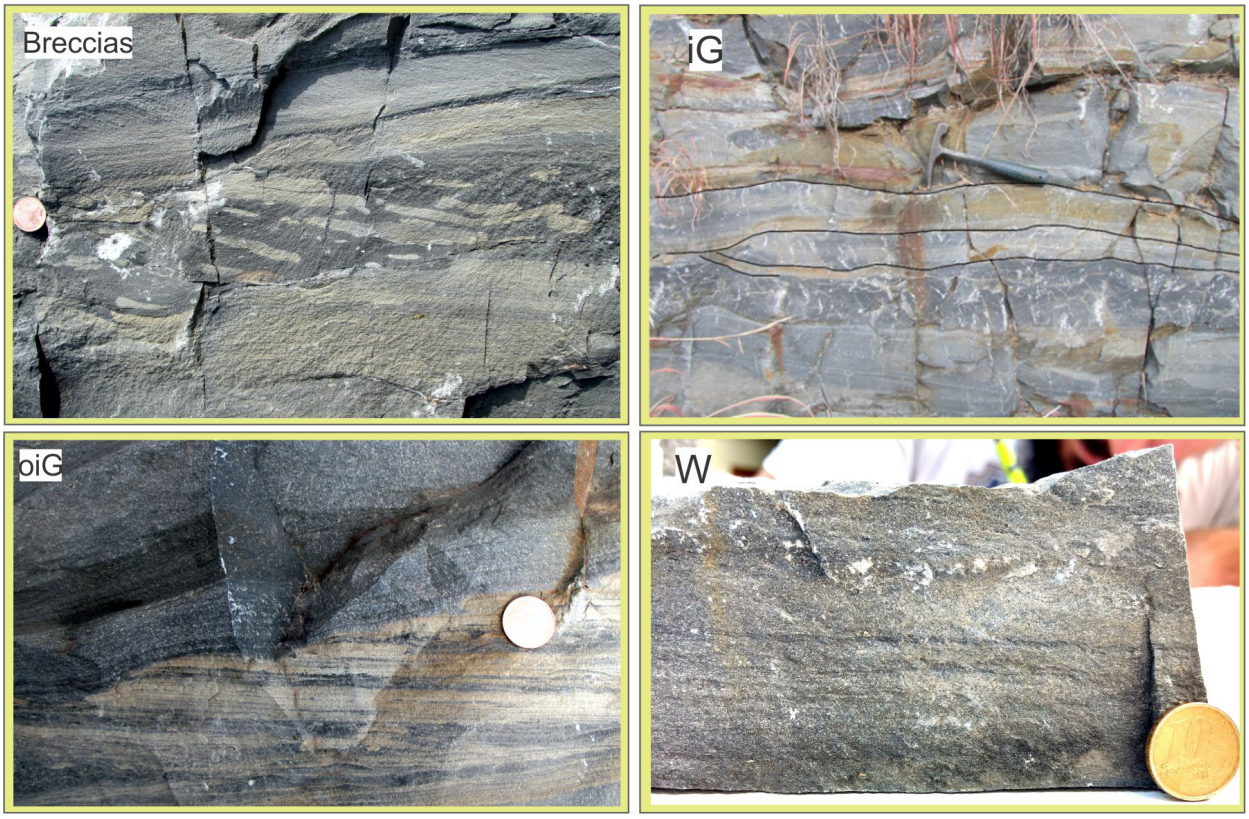

Figure 8. Theoretical tempestite facies correlated to lithofacies described for the Lagoa do Jacaré Formation in the GMD quarry. The most important lithofacies in the outcrop in detail: breccias (B), intraclastic grainstone (iG), oncoidal-ooidal grainstone (oiG). Wackestone with siliciclastic representing finer lithofacies.

conditions, important characteristics in order to understand stratigraphic depositional evolution. According to Aigner (1985), Einsele and Seilacher (1991), Molina *et al.* (1997), Mohseni and Al-Aasm (2004), Nichols (2009), Pérez-López and Pérez-Valera (2012) as well as other authors, structures like sharp boundaries, thin layers (1-5 cm), minor differences in composition, high content of lutite facies, localized hummocky cross-stratification, and ondulated top of the bed are diagnostic of a distal sedimentation environment (Figs. 4B, 4D and 4F). The lithofacies described in this paper fit the ones presented above and thus suggest that distal tempestite cycles generated in a carbonate ramp (ramp model of Burchette and Wright 1992) were mainly responsible for the deposition of the Lagoa do Jacaré Formation in the GMD quarry.

Carbonates from the middle Bambuí Group were formed in a conspicuously high energy marine environment that likely dominated the entire basin system at slightly different times. Storm-deposited beds are apparently a hallmark of the Lagoa do Jacaré Formation and although storm-influenced depositional facies are also important facies described in the GMD quarry, the upper part of the composite section, until the 913 m mark, presents a thick ooidal intraclastic grainstones and rudstones. They likely represent shoreface deposits in inner ramp, reworked by the action of constant fair-weather waves, intercalated with mudrock and sandstones. These coarser carbonate facies depict a remarkable change in the stratigraphic record, as explained below.

In a sequence stratigraphic context, the lower part of the section, from the base and up to the 892 m-mark, a regressive pattern is interpreted due to the occurrence of repeated tempestite facies capped by a 10 m-thick ooidal-oncoidal grainstone, shown in detail in Figures 3, 9 and 10. In this coarser interval, important changes in lithofacies were described, where ooids with carbonate fringes in a loose packing make up the main allochemical grains, presenting planar cross-stratification and beds with lenticular geometry. These characteristics are related to shallower marine environments (Fig. 9), similar to ooid shoals deposited parallel to the shoreline in the inner ramp, under the action of fair-weather waves (Jones 2010). A maximum regressive surface (MRS) is then positioned at the top of this regressive hemicycle.

Above this interval, the second part of the section has completely changed the depositional context, where fine sediments of likely deep marine environment are deposited. Siliciclastic rocks are common, with thick mudrock and sandstone intercalated with thin ooidal grainstone beds. The significant change from carbonate to a mixed siliciclastic-carbonate sedimentation likely marks the gradual transition from the Lagoa do Jacaré Formation to the Serra da Saudade Formation. The base of the latter is marked by the contact between the fine-grained sandstone bed and the ooidal rudstone in the 913 m-mark. It is possible that this contact is controlled by tectonic and/or climatic changes, working in tandem to change the sea level and control the intercalation between carbonate and siliciclastic inputs. Drier climate phases with lower continental runoff could enable the sedimentation of carbonates in the context of a mixed siliciclastic-carbonate sedimentation, such as the

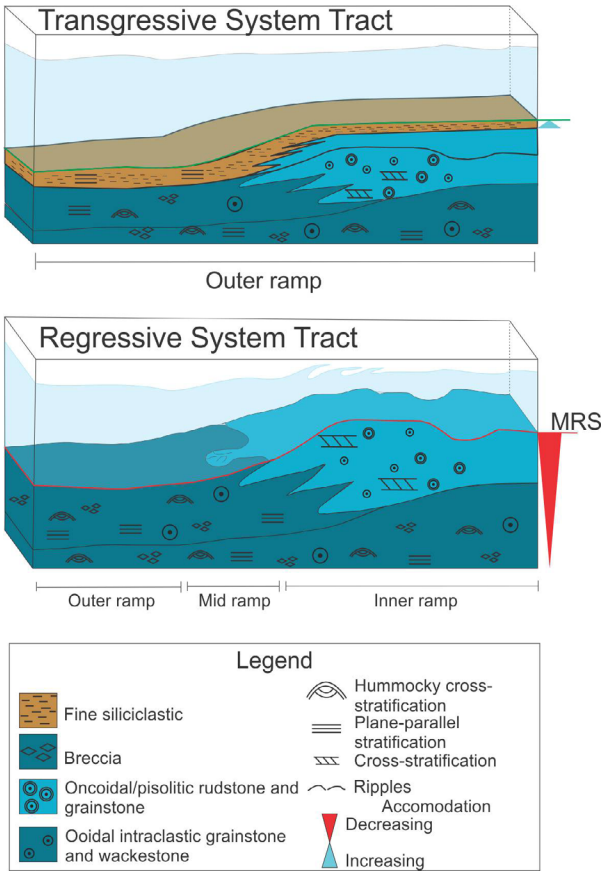

MRS: maximum regressive surface.

Figure 9. Depositional environment and sequence stratigraphy interpreted to the Lagoa do Jacaré Formation.

Sergipe-Alagoas Basin occurrence, where the sedimentation of encrusting algae and corals right above sandstones and conglomerates is well documented (Falcone 2006, Turbay *et al.* 2013, Dias-Brito and Tibana 2015). The entire interval from the 892 m-mark toward the top, marked at the base by the MRS, can be interpreted as part of the last regional drowning event of the Bambuí Basin that represents the end of the carbonate deposition, as shown in Caxito et al. (2018) and Uhlein *et al.* (2019), here described as a transgressive hemicycle.

The two hemicycles described above relate to higher frequency cycles. However, under a lower resolution approach, it is possible to set a single transgressive system tract to the entire section, which expresses the evolution from a mid/outer carbonate ramp represented by the Lagoa do Jacaré Formation to an offshore siliciclastic environment, represented by the Serra da Saudade Fm., as shown in Figure 9.

Geochemistry × depositional environment

In the studied section $\delta^{13}C$, values ranged from +11.11‰ to +13.94‰, and $\delta^{18}O$ values ranged from -10.94‰ to -5.94‰, with only three values lower than -10‰ , which is considered the limit for primary values (Fölling and Frimmel 2002) (Tab. 2).

Positive or negative correlations between C and O values have been widely used as a tool for the evaluation of post-depositional alteration of carbon isotopes in carbonate rocks, related to meteoric water burial diagenesis coupled with

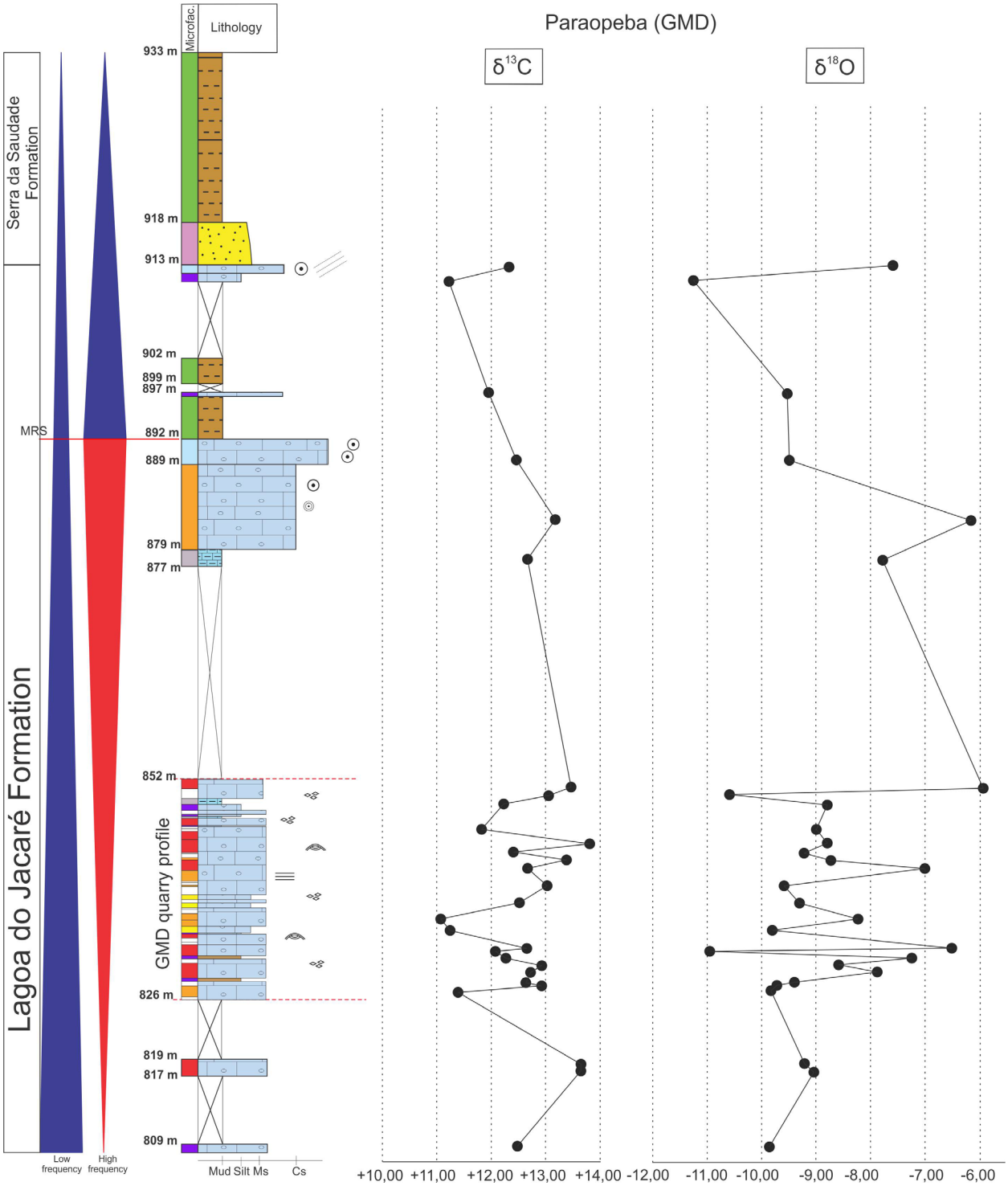

Figure 10. Interpreted composite vertical profile of the GMD quarry and surroundings in Paraopeba area. A regressive hemicycle at the lower part grading to a transgressive hemicycle at the top.

organic matter oxidation (Jacobsen and Kaufman 1999, Pandit *et al.* 2003). Elemental geochemistry is also commonly used to track possible alteration of isotopes, such as Mn/Sr and Mg/Ca ratios versus $\delta^{13}C$ data (e.g., Cui *et al.* 2018, Uhlein *et al.* 2019). Values obtained from our samples have a scattered distribution in a C and O isotopes cross-plot (Fig. 11), therefore suggesting little to no impact of post-depositional processes regarding this data. The coefficient of determination (R^2) for our entire data set is 0.104, however, if we look carefully, a certain genetic link between C and O isotopes is seen in different parts of the studied section. Samples above (877-973 m) and below (808-826 m) in the GMD quarry section have a correlation factor of 0.84 and 0.95, respectively, which could suggest possible pos-depositional alteration of the isotopic signal. One other option may be a case of subsampling. The main interval of the studied section has 20 samples in 26 m, almost a sample per meter, yielding a R^2 of only 0.05. Considering the upper interval of the section, we collected 6 samples in a 36 m-thick interval, making it one sample per 6 m. Consequently, its R^2 factor rises to 0.84 (Fig. 11). Taking into account these results and those particularities of the diagenetic evolution presented in the previous topic, the parameters

Table 2. C and O results.

Sample	m	$\delta^{13}C$	$\delta^{18}O$
PP09	809	12.496	-9.842
PP08B	815	13.651	-9.045
PP08A	819	13.679	-9.202
G4-16	826.4	11.43	-9.81
G4-15	827	12.98	-9.7
G4-14	827.8	12.73	-9.39
G4-12	830.1	12.82	-7.88
G4-11	831	12.99	-8.56
G4-9	832.8	12.31	-7.25
G4-8	833.6	12.12	-10.94
G4-7	834.3	12.72	-6.49
G4-4	836	11.26	-9.81
G4-2	837.3	11.11	-8.26
G5-1	839	12.65	-9.26
G5-2	839.6	13.08	-9.53
G5-4	841.9	12.77	-6.96
G5-5	842.9	13.54	-8.73
G5-6	844	12.52	-9.21
G5-7	844.7	13.94	-8.77
G5-11	847.7	11.92	-8.98
G5-14	849.7	12.31	-8.77
G5-15	851	13.14	-10.54
G5-16	852	13.56	-5.94
PP07	877	12.673	-7.767
PP06	881	13.169	-6.185
PP05C	892	12.46	-9.429
PP04A	901	11.957	-9.538
PP03	912	11.203	-11.251
PP02	913	12.329	-7.563

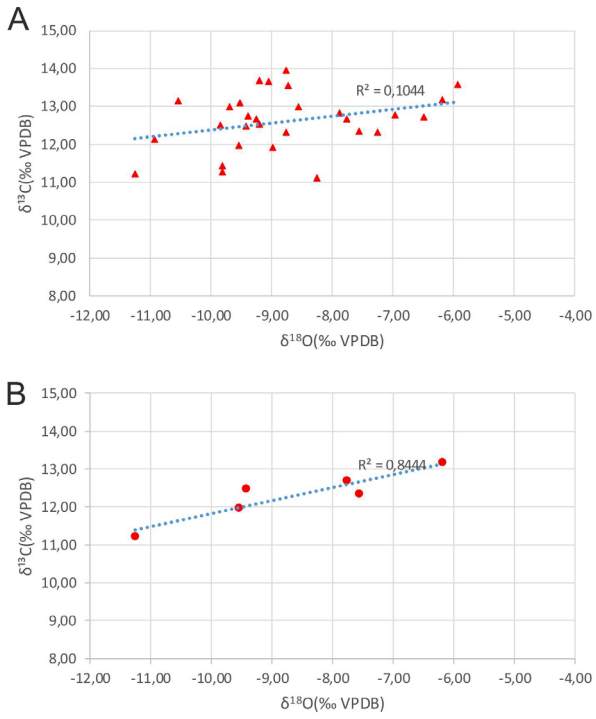

Figure 11. Values of C and O isotopes obtained in our samples: all samples in A and samples from 877-973 m interval in B.

already explained, and the similarity of the values with other studies, C and O isotopes from the GMD quarry studied here are likely primary, although some levels may have been lightly altered. From the 826 m to the 852 m-mark, there is a fluctuation of $\delta^{13}C$ values between +11.4 to +13.9‰. This is likely not linked to post-depositional processes (C and O correlation factor = 0.104; n = 11). Rather, this variation may reflect high-frequency changes in variables that rule the marine carbon cycle, such as the fraction of carbon buried as organic matter, the carbon isotope fractionation during photosynthesis, among others (e.g., Schrag *et al.* 2013, Cui *et al.* 2020).

Our facies descriptions and petrographic characterization show that primary macro and micro carbonate fabrics are well preserved. Due to those reasons, we were able to interpret a depositional setting of lower to middle shoreface frequently reworked by storm and fair-weather waves. Furthermore, the integrity of depositional and mineralogical features corroborates the interpretation that the highly positive $\delta^{13}C$ values are mainly of primary origin. In light of that, it is unlikely that burial diagenetic fluids interacted significantly with the sediments. Our data also show that the high $\delta^{13}C$ values occur throughout the section, regardless of sedimentary facies. The tendency of less positive $\delta^{13}C$ values from the base to the top as well as facies distributions are similar to the Lagoa do Jacaré Formation described in the northern portion of Minas Gerais (Uhlein *et al.* 2019). The GMD quarry carbonates here investigated represent the KM7-14 section of Cui *et al.* (2020) and therefore our novel sedimentologic, stratigraphic and isotopic data are complementary and go in unison toward primary physical and chemical characteristics for the Lagoa do Jacaré Formation and the MIBE.

The extremely high $\delta^{13}C$ values indicate an environment heavily depleted in ^{12}C in comparison to ^{13}C. In normal marine conditions, a small increase in $\delta^{13}C$ values may be explained by a high organic matter burial rate, consuming and insolating much of the marine water ^{12}C isotope (Rodrigues and Fauth 2013). However, based on a steady-state model, it is expected that almost 70% of organic carbon is buried in the sediments in order to achieve the highly positive $\delta^{13}C$ values of the Lagoa do Jacaré Formation (Uhlein *et al.* 2019, Cui *et al.* 2020, Caetano-Filho *et al.* 2021). As a simple comparison, this represents over 3 times the amount (i.e., ca. 20%) of organic carbon burial in the modern oceans. This scenario is unlikely since the carbonates and shales of the Lagoa do Jacaré Formation are lean in organic content (organic content < 0.2%, Uhlein *et al.* 2019, Cui *et al.* 2020) and the organic burial is self-limiting through the production of O_2 (and derived electron acceptors), creating negative feedback through enhanced respiration. Regarding the purported absence of high organic content levels, our up to date understanding of the middle Bambuí interval is limited by inner to outer ramp settings. Organic-rich facies may be present at the basin depocenter, far from the carbonate ramp context, being deposited simultaneously to the shallower carbonatic facies of the Lagoa do Jacaré Formation. As a starting point to this discussion, a well in the Janpovar region drilled by Petra Energia and provided by ANP (Brazilian National Petroleum Agency), in northern

Minas Gerais and 370 km northern of the GMD quarry, has logged the middle Bambuí interval (from the Serra de Santa Helena Formation to the lower Lagoa do Jacaré Formation), showing an extremely radioactive carbonate-shale succession (up to 320º API) (Fig. 12). At this interval, the core samples at the base of the Lagoa do Jacaré Fm. are described as micaceous, lightly calciferous dark grey shale with a high pyrite content. Since uranium is concentrated in organic constituents, black organic-rich shales tend to be more radioactive than most other shales (100º API; e.g., Doveton and Merriam 2004, Ellis and Singer 2008). Thus, the high radioactivity (average 165ºAPI) and core description of this interval (from 550 m to 300 m) fit to likely organic-rich shales and carbonates in the middle Bambuí interval. We understand that this is not a turning point to the interpretation of the highly positive $\delta^{13}C$ values, but it does suggest hidden basinal organic-rich facies below hundreds of meters of sedimentary rocks in basin distal areas, which must be further explored and eventually considered in future isotope modeling. Therefore, we suggest that a higher organic burial rate may help explaining the MIBE, acting in tandem with water column methanogenesis and reworking of ancient carbonate platforms, as previously suggested by Uhlein *et al.* (2019), Cui *et al.* (2020) and Caetano-Filho *et al.* (2021).

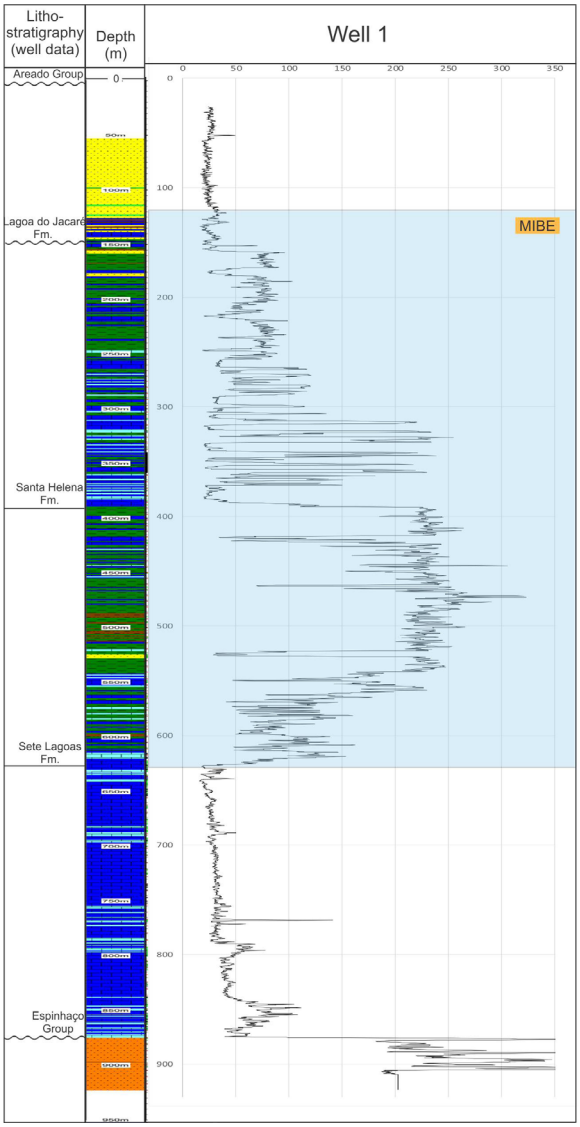

Figure 12. Well 1, located in northern Minas Gerais. The black line represents total gamma-ray in ºAPI.

Although it was never investigated in detail in terms of depositional facies, the Lagoa do Jacaré Formation shows features from storm-deposited beds to peritidal microbialites (e.g., Santos *et al.* 2018, Uhlein *et al.* 2019, Freitas *et al.* 2021), depicting a completely structured ancient carbonate ramp that likely covered hundreds of thousands of square kilometers. A restrictive, anoxic, and methanogenic basin during this time is hypothesized by many authors (e.g. Martins and Lemos 2007, Uhlein *et al.* 2019, Cui *et al.* 2020, Caetano-Filho *et al.* 2021) mainly from stable isotopes evidence. The methanogenic basin model from Cui *et al.* (2020) and Caetano-Filho *et al.* (2021) proposes a restricted and likely fully anoxic basin water, in which the methanogenic zone occurs up the water column. From inner ramp to deep basin settings, the produced and exported organic carbon may be subjected to methanogens population.

However, it is expected the development and maintenance of a well-mixed and likely oxic surface water layer that should be an efficient zone of rapid aerobic methane oxidation for a late Ediacaran ramp highly influenced by storm events and yielding oolitic shoals and lagoonal facies. (e.g., Carini *et al.* 2005). The process of methanotrophy, if relevant, would then become a conflict to the model proposed by Cui *et al.* (2020) and Caetano-Filho *et al.* (2021). Thus, it is relevant to the understanding of the MIBE that stratigraphic stacking patterns, facies associations and depositional settings of the shallow and deep facies of the MIBE are properly interpreted and associated to the novel geochemical tools that should be applied in the near future.

CONCLUSIONS

This work provides carbonate facies description, and a chemostratigraphic profile of part of the Lagoa do Jacaré Formation, Bambuí Group, in the region of Paraopeba, central Brazil. Storm-wave sedimentary facies (tempestite cycles) were detailed relating to the occurrence of nine lithofacies in the GMD quarry and surroundings. High-energy micro- and macrofacies were described at the base, grading upward to low energy facies in a storm-dominated carbonate ramp. The occurrence of shallower ooidal facies was also described, grading to deep marine siliciclastic sediments at the top.

Stratigraphic analysis provided the interpretation of two high-frequency hemicycles in a 124 m-thick section, making up a transgressive hemicycle in a lower frequency. This interpretation is in line with the general drowning trend expected within the changes from the Lagoa do Jacaré Formation (carbonate ramp with wave action) to the Serra da Saudade Formation (siliciclastic deep marine).

New $\delta^{13}C$ and $\delta^{18}O$ isotopic data from an interval exposed in the GMD quarry region was also presented, bringing new light to the previous interpretations of this unit's isotopic signal. Highly positive $\delta^{13}C$ values are still considered to be caused by a highly restricted marine environment, but well log data

evidence of local high rates of organic matter burial is highlighted. The investigation of similar organic-rich intervals and U content in other well logs is proposed.

ACKNOWLEDGEMENTS

The authors are grateful to the Universidade Federal de Minas Gerais (UFMG), Universidade Federal de Sergipe (UFS) and ANP/Petrobras (Project CAMURES-Diagênese/FUNDEP 5850.0106111.17.9) for funding and releasing data. We also thank the Universidade Federal de Pernambuco and Universidade do Estado do Rio de Janeiro for isotope analyses. MVSD thanks the Coordenação de Aperfeiçoamento de Pessoal de Nível Superior (CAPES) for scholarship. The authors also thank anonymous reviewers to comments and suggestions that actually improved the quality of the original manuscript.

ARTICLE INFORMATION

Manuscript ID: 20200135. Received on: 29 DEC 2020. Approved on: 29 NOV 2021.

How to cite this article: Dantas M.V.S., Uhlein A., Uhlein G.J., Freitas A.R., Mendonça T.K., Santos J.A.O., Silva S.A.M. Carbonate storm deposits and C, O isotopes of the Lagoa do Jacaré Formation (Ediacaran) in the Paraopeba area, Bambuí Group, Brazil. *Brazilian Journal of Geology*, 52(1):e20200135, 2022. https://doi.org/10.1590/2317-4889202120200135.

M.D. is the leader, therefore wrote the first draft of the manuscript and prepared all figures; G.U. provided main discussions about geochemistryand also detailed English language review. A.U. is the advisor and coordinates the development of the main ideas of the manuscript and writing of regional geology and fieldwork data interpretation. T.K. and A.R. participated in the fieldwork and collecting data, in addition to collaborating in petrographic descriptions and discussions. J.A. made significant contributions to diagenesis evaluation. S.A. contributed to fieldwork campaigning and sample description.

Competing interests: the authors declare no competing interests.

REFERENCES

Aigner T. 1985. Storm depositional systems. Lecture Notes in Earth Sciences. Berlin: Springer Verlag, 174 pp.

Alkmin F.F., Martins-Neto M.A. 2001. A Bacia Intracratônica do São Francisco: Arcabouço estrutural e cenários evolutivos. In: Martins-Neto M.A., Pinto C.P. (Eds.). *Bacia do São Francisco*. Geologia e Recursos Minerais. Belo Horizonte: SBG/MG, p. 9-30.

Alkmim F.F., Martins-Neto M.A. 2012. Proterozoic first-order sedimentary sequences of the São Francisco craton, eastern Brazil. *Marine and Petroleum Geology*, 33(1):127-139. https://doi.org/10.1016/j.marpetgeo.2011.08.011

Alvarenga C.J.S., Dardenne M.A., Vieira L.C., Martinho C.T., Guimarães E.M., Santos R.V., Santana R.O. 2012. Estratigrafia da borda ocidental da Bacia do São Francisco. *Boletim de Geociências da Petrobras*, 20(1-2):145-164.

Alvarenga C.J.S., Della Giustina M.E.S., Silva M.G.C., Santos R.V., Gioia S.M.C., Guimarães E.M., Dardenne M.A., Sial A.N., Ferreira V.P. 2007. Variações dos isótopos de C e Sr em carbonatos pré e pós-glaciação Jequitaí (Esturtiano) na região de Bezerra-Formosa, Goiás. *Revista Brasileira de Geociências*, 37(4):147-155.

Babinski M., Vieira L.C., Trindade R.I.F. 2007. Direct dating of the Sete Lagoas cap carbonate (Bambuí Group, Brazil) and implications for the Neoproterozoic glacial events. *Terra Nova*, 19(6):401-406. https://doi.org/10.1111/j.1365-3121.2007.00764.x

Brenchley P.J. 1985. Storm influenced sandstone beds. *Modern Geology*, 9:369-396.

Burchette T.P., Wright V.P. 1992. Carbonate ramp depositional systems. *Sedimentary Geology*, 79(1-4):3-57. https://doi.org/10.1016/0037-0738(92)90003-A

Caetano-Filho S., Sansjofre P., Ader M., Paula-Santos G.M., Guacaneme C., Babinski M., Bedoya-Rueda C., Kuchenbecker M., Reis H.L.S., Trindade R.I.F. 2021. A large epeiric methanogenic Bambuí sea in the core of Gondwana supercontinent? *Geoscience Frontiers*, 12(1):203-218. https://doi.org/10.1016/j.gsf.2020.04.005

Carini S., Bano N., LeCleir G., Joye S.B. 2005. Aerobic methane oxidation and methanotroph community composition during seasonal stratification in Mono Lake, California (USA). *Environmental Microbiology*, 7(8):1127-1138. https://doi.org/10.1111/j.1462-2920.2005.00786.x

Castro P.T.A., Dardenne M.A. 2000. The sedimentology, stratigraphy and tectonic context of the São Francisco Supergroup at the southern boundary of the São Francisco craton, Brazil. *Revista Brasileira de Geociências*, 30(3):345-437.

Caxito F.A., Frei R., Uhlein G.J., Dias T.G., Árting T.B., Uhlein A. 2018. Multiproxy geochemical and isotope stratigraphy records of a neoproterozoic oxygenation even tin the Ediacaran Sete Lagoas cap carbonate, Bambuí Group, Brazil. *Chemical Geology*, 481:119-132. https://doi.org/10.1016/j.chemgeo.2018.02.007

Caxito F.A., Halverson G.P., Uhlein A., Stevenson R., Dias T.G., Uhlein G.J. 2012. Marinoan glaciation in east central Brazil. *Precambrian Research*, 200-203:38-58. https://doi.org/10.1016/j.precamres.2012.01.005

Cloud P., Dardenne M.A. 1973. Proterozoic age of the Bambuí Group in Brazil. *Geological Society of America Bulletin*, 84(5):1673-1676. https://doi.org/10.1130/0016-7606(1973)84%3C1673:PAOTBG%3E2.0.CO;2

Coelho J.C.C., Martins-Neto M.A., Marinho M.S. 2008. Estilos estruturais e evolução tectônica da porção mineira da bacia proterozoica do São Francisco. *Revista Brasileira de Geociências*, 38(Suppl. 2):149-165.

Condie K.C. 2016. *Earth as an evolving planetary system*. San Diego: Elsevier, 436 p.

Cordani U.G., Kawashita K., Thomaz Filho A. 1978. Applicability of the rubidium-strontium method to shales and related rocks. *Studies in Geology*, 6:93-117.

Cui H., Kaufman A.J., Peng Y., Liu X., Plummer R.E., Lee E.I. 2018. The Neoproterozoic Hüttenberg δ13C anomaly: Genesis and global implications. *Precambrian Research*, 313:242-262. https://doi.org/10.1016/j.precamres.2018.05.024

Cui H., Warren L.V., Uhlein G.J., Okubo J., Liu X., Plummer R.E., Baele J., Goderis S., Claeys P., Li F. 2020. Global or local? Constraining the origins of the middle Bambuí carbon cycle anomaly in Brazil. *Precambrian Research*, 348:105861. https://doi.org/10.1016/j.precamres.2020.105861

Dardenne M.A. 1978. Síntese sobre a estratigrafia do Grupo Bambuí no Brasil Central. *In*: Congresso Brasileiro de Geologia, 30., 1978, Recife. *Proceedings*... v. 2, p. 507-610.

Dardenne M.A. 2000. The Brasília fold belt. *In*: Cordani U.G., Milani E.J., Thomaz Filho A., Campos D.A. (Eds.) *Tectonic Evolution of South America*. Rio de Janeiro: 31st International Geological Congress, p. 231-264.

Dias-Brito D. 2017. *Guia petrográfico dos carbonatos do Brasil*. Rio Claro: UNESP, 232 p.

Dias-Brito D., Tibana, P. 2015. *Calcários do cretáceo do Brasil*. Rio Claro: UNESP, 576 p.

Doveton J.H., Merriam D.F. 2004. Borehole petrophysical chemostratigraphy of Pennsylvanian black shales in the Kansas subsurface. *Chemical Geology*, 206(3-4):249-258. https://doi.org/10.1016/j.chemgeo.2003.12.027

Dunham R.J. 1962. Classification of carbonate rocks according to their depositional texture. *In*: Ham W.E. (Ed.). *Classification of Carbonate Rocks:* a symposium. Tulsa: American Association of Petroleum Geologists Memoir, 1:108-121.

Einsele G. 1992. *Sedimentary basins:* evolution, facies and sedimentary budget. Berlin: Spring-Verlag, 628 p.

Einsele G., Seilacher A. 1991. Distinction of tempestites and turbidites. *In*: Einsele G., Ricken W., Seilacher A. (Eds.). *Cycles and events in stratification*. Heidelberg-New York: Springer, p. 377-382.

Ellis D.V., Singer J.M. 2008. *Well logging for Earth scientists*. 2ª ed. Berlin: Springer.

Embry A.F., Johannessen E.P. 1993. T-R sequence stratigraphy, facies analysis and reservoir distribution in the uppermost Triassic Lower Jurassic succession, western Sverdrup Basin, Arctic Canada. *Norwegian Petroleum Society Special Publication*, 2:121-146.

Embry A.F., Klovan J.E. 1971. A Late Devonian reef tract on northeastern Banks Island, N.W.T. *Bulletin of Canadian Petroleum Geology*, 19(4):730-781. https://doi.org/10.35767/gscpgbull.19.4.730

Falcone C.M.O. 2006. *Sedimentação mista carbonato-siliciclástico durante o Albo-aptiano na porção emersa da Bacia Sergipe-Alagoas*. PhD Thesis, Universidade do Vale do Rio dos Sinos, São Leopoldo, 193 p.

Flügel E. 2010. *Microfacies of carbonate rocks:* analysis, interpretation and application. Berlin: Springer-Verlag, 976 p.

Fölling P.G., Frimmel H.E. 2002. Chemostratigraphic correlation of carbonate successions in the Gariep and Saldania Belts, Namibia and South Africa. *Basin Research*, 14(1):69-88. https://doi.org/10.1046/j.1365-2117.2002.00167.x

Fragoso D.G., Uhlein A., Sanglard J.C., Suckau G.L., Guerzoni H.T., Faria P.H. 2011. Geologia dos Grupos Bambuí, Areado e Mata da Corda na folha de Presidente Olegário (1:100.000), MG: registro deposicional do Neoproterozoico ao Neocretáceo da Bacia do São Francisco. *Geonomos*, 19(1):28-38. https://doi.org/10.18285/geonomos.v19i1.60

Freitas A.R., Uhlein A., Dantas M.V.S., Mendonça T.K. 2021. Caracterização em multiescala de carbonatos neoproterozóicos da Pedreira GMD, Formação Lagoa do Jacaré, Grupo Bambuí, Paraopeba-MG. *Geologia USP. Série Científica*, 21(1):103-120. https://doi.org/10.11606/issn.2316-9095.v21-163573

Hippert J.P., Caxito F.A., Uhlein G.J., Nalini H.A., Sial A.N., Abreu A.T., Nogueira L.B. 2019. The fate of a Neoproterozoic intracratonic marine basin: Trace elements, TOC and IRON speciation geochemistry of the Bambuí Basin, Brazil. *Precambrian Research*, 330:101-120. https://doi.org/10.1016/j.precamres.2019.05.001

Hoffman P.F., Kaufman A.J., Halverson G.P., Schrag D.P. 1998. A Neoproterozoic snowball Earth. *Science*, 281(5381):1342-1346. https://doi.org/10.1126/science.281.5381.1342

Iyer S.S., Babinski M., Krouse H.R, Chemale Jr. F. 1995. Highly 13C[enriched carbonate and organic matter in the Neoproterozoic sediments of the Bambuí Group, Brazil. *Precambrian Research*, 73:271-282.

Jacobsen S.B., Kaufman A.J. 1999. The Sr, C and O isotopic evolution of Neoproterozoic seawater. *Chemical Geology*, 161:37-57.

Jones B. 2010. Warm-water neritic carbonates. *In*: James N.P., Dalrymple R.W. (Eds.). *Facies Models 4*. Canada: Geological Association of Canada, p. 167-200.

Johnston D.T., Macdonald F.A., Gill B.C., Hoffman P.F., Schrag D.P. 2012. Uncoveringthe Neoproterozoic carbon cycle. *Nature*, 483(7389):320-323. https://doi.org/10.1038/nature10854

Kuchenbecker M., Babinski M., Pedrosa-Soares A.C., Lopes-Silva L., Pimenta F. 2016. Chemostratigraphy of the lower Bambuí Group, southwestern São Francisco craton, Brazil: insights on Gondwana paleoenvironments. *Brazilian Journal of Geology*, 46(Suppl. 1):145-162. https://doi.org/10.1590/2317-488920160030285

Li C., Hardisty D.S., Luo G., Huang J., Algeo T.J., Cheng M., Shi W., An Z., Tong J., Xie S., Jiao N., Lyons T.W. 2016. Uncovering the spatial heterogeneity of Ediacarancarbon cycling. *Geobiology*, 15(2):211-224. https://doi.org/10.1111/gbi.12222

Martins M., Lemos V.B. 2007. Análise estratigráfica das sequências neoproterozoicas da Bacia do São Francisco. *Revista Brasileira de Geociências*, 37(4):156-167.

Martins-Neto M.A., Pedrosa-Soares A.C., Lima S.A.A. 2001. Tectono-sedimentary evolution of sedimentary basis from Late Paleoproterozoic to Late Neoproterozoic in the São Francisco craton and Araçuaí fold belt, eastern Brazil. *Sedimentary Geology*, 141-142:343-370. https://doi.org/10.1016/S0037-0738(01)00082-3

Mohseni H., Al-Aasm I.S. 2004. Tempestite deposits on a shore-influenced carbonate ramp: an example from the Pabdeh Formation (Paleogene), Zagros basin, SW Iran. *Journal of Petroleum Geology*, 27(2):163-178. https://doi.org/10.1111/j.1747-5457.2004.tb00051.x

Molina J.M., Ruiz-Ortiz P.A., Vera J.A. 1997. Calcareous tempestites in pelagic facies (Jurassic, Beltic Cordilleras, Southern Spain). *Sedimentary Geology*, 109(1-2):95-109. https://doi.org/10.1016/S0037-0738(96)00057-7

Moreira D.S., Uhlein A., Dussin I.A., Uhlein G.J., Misuzaki A.M.P. 2020. A Cambrian age for the upper Bambuí Group, Brazil, supported by the first U-Pb dating of volcaniclastic bed. *Journal of South American Earth Sciences*, 99:102503. https://doi.org/10.1016/j.jsames.2020.102503

Myrow P.M., Southard J.B. 1996. Tempestite deposition. *Journal of Sedimentary Research*, 66(5):875-887. https://doi.org/10.1306/D426842D-2B26-11D7-8648000102C1865D

Nichols G. 2009. *Sedimentology and stratigraphy*. 2. ed. Chichester: Wiley-Blackwell, 419 p.

Pandit M.K., Sial A.N., Malhotra G., Shekhawat L.S., Ferreira V.P. 2003. C-, O- Isotope and Whole-rock Geochemistry of Proterozoic Jahazpur Carbonates, NW Indian Craton. *Gondwana Research*, 6(3):513-522.

Parenti-Couto J.G., Cordani U.G., Kawashita K., Iyer S.S., Moraes N.M.P. 1981. Considerações sobre a idade do Grupo Bambuí, com base em análises isotópicas de Sr e Pb. *Revista Brasileira de Geociências*, 11(1):5-16.

Paula-Santos G.M., Caetano-Filho S., Babinski M., Trindade R.I., Guacaneme C. 2017. Tracking connection and restriction of West Gondwana São Francisco Basin through isotope chemostratigraphy. *Gondwana Research*, 42:280-305. https://doi.org/10.1016/j.gr.2016.10.012

Paula-Santos G.V., Babinski M., Kuchenbecker M., Caetano-Filho S., Trindade R.I., Pedrosa-Soares A.C. 2015. New evidence of an Ediacaran age for the Bambuí Group in southern São Francisco craton (eastern Brazil) from zircon U–Pb data and isotope chemostratigraphy. *Gondwana Research*, 28(2):702-720. https://doi.org/10.1016/j.gr.2014.07.012

Pérez-López A., Pérez-Valera F. 2012. Tempestite facies models for the epicontinental Triassic carbonates of the Betic Cordillera (southern Spain). *Sedimentology*, 59(2):646-678. https://doi.org/10.1111/j.1365-3091.2011.01270.x

Pimentel M.M., Rodrigues J.B., Della Giustina M.E.S., Junges S., Matteini M., Armstrong R. 2011. The tectonic evolution of the Neoproterozoic Brasília Belt, central Brazil, based on SHRIMP and LA–ICPMS U–Pb sedimentary provenance data: a review. *Journal of South America Earth Sciences*, 31:345-357.

Reis C. 2013. *Geologia, sistemas deposicionais e estratigrafia isotópica do Grupo Bambuí na região de Santa Maria da Vitória, BA*. MS Dissertation, Instituto de Geociências, Universidade de Brasília, Brasília, 97 p.

Reis H.L.S., Alkmim F.F. 2015. Anatomy of a basin-controlled foreland fold-thrust belt curve: The Três Marias salient, São Francisco basin, Brazil. *Marine and Petroleum Geology*, 66(4):711-731. https://doi.org/10.1016/j.marpetgeo.2015.07.013

Reis H.L.S, Alkmim F.F., Fonseca R.C.S., Nascimento T.C., Suss J.F., Prevatti L.D. 2017. The São Francisco Basin. *In*: Heilbron M., Cordani U.G., Alkmim F.F. (Eds.). São Francisco Craton, Eastern Brazil. *Regional Geology Reviews*, Switzerland: Springer International, p. 117-143. https://doi.org/10.1007/978-3-319-01715-0_7

Reis H.L.S., Fonseca R.C.S., Alkmim F.F., Nascimento T.C., Suss J. 2013. A Bacia do São Francisco (MG): registro de uma longa história de ativações e reativações em domínio cratônico. *In*: Simpósio de Geologia de Minas Gerais, 17.; Simpósio de Geologia do Sudeste, 13., Sociedade Brasileira de Geologia. *Proceedings*... Juiz de Fora: Sociedade Brasileira de Geologia.

Reis H.L.S., Suss J.F. 2016. Mixed carbonate-siliciclastic sedimentation in forebulgegrabens: an example from the Ediacaran Bambuí Group, São Francisco Basin, Brazil. *Sedimentary Geology*, 339:83-103. https://doi.org/10.1016/j.sedgeo.2016.04.004

Rodrigues G.B, Fauth G. 2013. Isótopos estáveis de carbono e oxigênio em ostracodes do Cretáceo: metodologias, aplicações e desafios. *Terrae Didatica*, 9(1):34-49. https://doi.org/10.20396/td.v9i1.8637408

Rodrigues J.B. 2008. *Proveniência de sedimentos dos grupos Canastra, Ibiá, Vazante e Bambuí – um estudo de zircões detríticos e Idades Modelo Sm–Nd*. PhD Thesis, Instituto de Geociências, Universidade de Brasília, Brasília, 128 p.

Santana R.O. 2011. *Estratigrafia, geoquímica e isótopos de C, O e Sr do Grupo Bambuí a leste da Falha de São Domingos, NE de Minas Gerais*. MS Dissertation, Instituto de Geociências, Universidade de Brasília, Brasília, 93 p.

Santos D.M., Sanchez E.A., Santucci R.M. 2018. Morphological and petrographic analysis of identified stromatolitic occurrences in Lagoa do Jacaré Formation, Bambuí Group, state of Minas Gerais, Brazil. *Journal of the Brazilian Society of Paleontology*, 21(3):195-207. https://doi.org/10.4072/rbp.2018.3.01

Santos R.V., Alvarenga C.J.S., Babinski M., Ramos M.L.S., Cukrov N., Fonseca M.A., Sial A.N., Dardenne M.A., Noce C.M. 2004. Carbon isotopes of Mesoproterozoic-Neoproterozoic sequences from Southern São Francisco craton and Araçuaí Belt, Brazil: Paleographic implications. *Journal of South American Earth Science*, 18(1):27-39. https://doi.org/10.1016/j.jsames.2004.08.009

Santos R.V., Alvarenga C.J.S., Dardenne M.A., Sial A.N., Ferreira V.P. 2000. Carbon and oxygen isotope profiles across Meso-Neoproterozoic limestones from central Brazil: Bambuí and Paranoá groups. *Precambrian Research*, 104(3-4):107-122. https://doi.org/10.1016/S0301-9268(00)00082-6

Schrag D.P., Higgins J.A., Macdonald F.A., Johnston D.T. 2013. Authigenic carbonate and the history of the global carbon cycle. *Science*, 339(6119):540-543. https://doi.org/10.1126/science.1229578

Sial A.N., Dardenne M.A., Misi A., Pedreira A.J., Gaucher C., Ferreira V.P., Silva Filho M.A., Uhlein A., Pedrosa-Soares A.C., Santos R.V., Egydio-Silva M., Babinski M., Alvarenga C.J.S., Fairchild T.R., Pimentel M.M. 2009. The São Francisco Palaeocontinent. *In*: Gaucher C., Sial A.N., Halverson G.P., Frimmel H.E. (Eds.). Neoproterozoic-Cambrian Tectonics, Global Change and Evolution: a focus on southwestern Gondwana. *Developments in Precambrian Geology*, 16. Amsterdam: Elsevier, p. 31-69.

Sial A.N., Gaucher C., Misi A., Boggiani P.C., Alvarenga C.J.S., Ferreira V.P., Pimentel M.M., Pedreira J.A., Warren L.V., Fernández-Ramírez R., Geraldes M., Pereira N.S., Chiglino L., Cezario W.S. 2016. Correlations of some Neoproterozoic carbonate-dominated successions in South America based on high-resolution chemostratigraphy. *Brazilian Journal of Geology*, 46(3):439-488. https://doi.org/10.1590/2317-4889201620160079

Taylor K.G., Macquaker J.H.S. 2000. Early diagenetic pyrite morphology in a mudstone-dominated succession: the Lower Jurassic Cleveland Ironstone Formation, eastern England. *Sedimentary Geology*, 131(1-2):77-86. https://doi.org/10.1016%2FS0037-0738(00)00002-6

Tuller M.P. (Coord.). 2010. *Projeto Sete Lagoas-Abaeté – Folha Sete Lagoas (SE.23-C-Z-II)*. Belo Horizonte: Serviço Geológico do Brasil, 160 p.

Turbay C.V.G., Cesero P., Garcia A.J.V., Silva R.C. 2013. Depositional, diagenetic and stratigraphic aspects of microfacies from Riachuelo Formation, Albian, Sergipe Basin, Brazil. *Geologia USP. Série Científica*, 13(4):29-48. https://doi.org/10.5327/Z1519-874X201300040002

Uhlein G.J., Uhlein A., Pereira E., Caxito F.A., Okubo J., Warren L.V., Sial A.N. 2019. Ediacaran paleoenvironmental changes recorded in the mixed carbonate siliciclastic Bambuí Basin, Brazil. *Palaeogeography, Palaeoclimatology, Palaeoecology*, 517:39-51. https://doi.org/10.1016/j.palaeo.2018.12.022

Uhlein G.J., Uhlein A., Stevenson R., Halverson G.P., Caxito F.A., Cox G.M. 2017. Early to Late Ediacaran conglomeratic wedges from a complete foreland basin cycle in the southwest São Francisco Craton, Bambuí Group, Brazil. *Precambrian Research*, 299:101-116. https://doi.org/10.1016/j.precamres.2017.07.020

Vieira L.C., Nédélec A., Fabre S., Trindade R.I.F., Almeida R.P. 2015. Aragonite crystalfans in Neoproterozoic cap carbonates: a case study from Brazil and implications for the post-snowball earth coastal environment. *Journal of Sedimentary Research*, 85(3):285-300. https://doi.org/10.2110/jsr.2015.21

Warren L.V., Quaglio F., Riccomini C., Simões M.G., Poiré D.G., Strikis N.M., Anelli L.E., Strikis P.C. 2014. The puzzle assembled: Ediacaran guide fossil Cloudina reveals an old proto-Gondwana seaway. *Geology*, 42(5):391-394. https://doi.org/10.1130/G35304.1

Zalán P.V., Romeiro-Silva P.C. 2007. Bacia do São Francisco. *Boletim de Geociências da Petrobras*, 15(2):561-571.

Zecchin M., Catuneanu O. 2017. High-resolution sequence stratigraphy of clastic shelves VI: Mixed siliciclastic-carbonate systems. *Marine and Petroleum Geology*, 88:712-723. https://doi.org/10.1016/j.marpetgeo.2017.09.012